# *Original Research Article*

## Solvo-thermal Assisted-Synthesis; Experimental and Theoretical Characterization; and Biological Evaluations of Azo-Chelator-Ligand Chelates of Fe(II) and Zn(II) ions


## Abstract

**Background and Objectives:**The resistance of microbes against anti-bacteriological drugs leading to countless deaths and terminal ailments remains a basis for concern.Hence, the main interest of this study was to design, synthesize and report unusual compounds with basic hydrophilic moieties plus hydrophobic functions. **Materials and Methods**: Analytical (melting points, micro-analysis (C. H.N.S) magnetic susceptibility ($\mu_{eff}$), molar conductance plus solubility test) methods; spectral (Fourier Transform Infrared(FTIR)), electrospray ionization mass spectrometry (ESI-MS), nuclear magnetic resonance ($^{1}$H- plus $^{13}$C-NMR), electronic(UV-Vis)) measurements; theoretical (DFT) evaluations were utilized for the characterization of the chelator and its chelates. All synthesized compounds were examined for antimicrobial and antioxidant potentials while the chelator was singly evaluated for solvent extractive capacity. **Results**: A nitrogenous based chelator-ligand, (E)-1-(((4,6-dimethylpyrimidin-2-yl)imino)methyl)naphthalen-2-ol(LH) synthesized throughreflux-condensation reaction of 2-amino-4,6-dimethylpyrimidine with 2-hydroxy-1-napthaldehyde was acquired. Further refluxof the chelator-ligand withbivalentions of iron-sulphate and zinc-acetate salts plus 2,2'-bipyridine resulted into separatebivalent-heterolepticmetallic chelates. The deprotonated nitrogen of the amine moiety and carbon of the carbonyl gave rise to the chelator-ligand with $N_2O_2$chromophoredetected around the metallic atom in the chelates. The $\mu_{eff}$data plusUV-Vis spectral values of the chelates conformed to 6-coordinate octahedral geometry. All the chelates were high spin and non-ionic in dimethylsulfoxide (DMSO). The antimicrobial and antioxidant screening of the compounds presented moderate to fantastic results, while the metallic extractive proficiency of the chelator showed outstanding extractability for $Fe^{2+}$ and $Zn^{2+}$ions with an efficiency of 79.34% and 51.92% correspondingly.**Conclusion**: All the synthesized compounds are novel and demonstrated prospective biological, plus metallic ions' extractive potentials required for designs plus isolation of products also for such actions.



**Keywords:** Pyrimidine, DFT Studies,Chelator-ligand, Chelates, Solvo-thermal synthesis


## 1. INTRODUCTION

Research undertakings on the improvement of metallic based antimicrobial drugs have had reasonablebreakthroughs over the years. However, drug resilientbacteriologicalorganismshas remained of utmost scientific concerns[1]. Countless metallic-based medications[2] have been prepared as well asevaluated against manifold drug resistingmicrobes[3]like methicillin resistant *Staphylococcus aureus,* vancomycin resistant *E. faecium* and penicillin resistant *S. pneumoniae* strains[4], however, with only few making it to preclinical trials. The major challenge lies with the risk of metal poisoning due to high level of toxicity among metal based drugs[5]. Hence, the focus in the growth of more operative anti-

bacteriologicalas well as anti-fungiform drugs is to synthesize drugs with broad spectrum antimicrobial potentials; of low toxicity, that can easily diffuse across microbial intracellular membrane, improved selectivity and with novel mechanisms of action[6].

The workability of anti-bacterial activities for most anti-bacteriological drugs remains a basisfor their attraction[7]to the transpeptidase target enzyme within the bacteria, potential to permeate the bacterial cell membrane in addition to the grade of openness to β-lactamases emitted by certainmicrobial strains like*Klebsillepnemonie*for detoxification drugs[8, 9].For enhancement of the aforementionedpotentials, our interest remainsto designunusual compounds with basic hydrophilic moieties[7]; OH, NH, $NH_2$, $CO_2H$ thatstimulateslipophilicity of drugsvia lipid cell membrane of countlessmicroorganisms, as well as drugs having hydrophobic functions; C=N, -$CH_2$-, C=Cwhich triggers sensitivity amid resistant Gram positive microbial strains[9]

Pyrimidine based compounds are acknowledged for excellent potentials in stabilizing biomolecules[10, 11] that could be used as connectors in organic synthesis and good ligating ability in the formation of metal complexes[12]. Metallic chelates encompassingpyrimidinylfunction groupare known to demonstrateexceptional antimicrobial actions,a consequence of their interesting topologies, assemblage liability, selectivity to countless molecular environs, capability to displayinfrequentgeometries unusual to resistant bacteria as well as their capacity to avertprompted oxidative stress damages[13]. This work reported the solvo-thermal assisted-synthesisnew azo-chelator-ligand with its Fe(II) and Zn(II) chelates. The experimental and theoretical characterization in addition to the efficiency of the compounds as broad-spectrum *in vitro* antimicrobial agents were separately appraised

## 2. MATERIALS AND METHODS

### 2.1 MATERIALS

The reagents/solvents adopted for this research without further purification were acquired from Merck o, Sigma-Aldrich o., and ACE Co. All the experimental works of this study were carried out at the research laboratory of the Department of Chemistry, Ignatius Ajuru Universityof Education, Rivers State, Nigeria form February-July, 2021.

### 2.2 SYNTHESIS AND PHYSICAL MEASUREMENTS

The chelator-ligand, ((E)-1-(((4,6-dimethylpyrimidin-2-yl)imino)methyl)naphthalen-2-ol); and its metallic-chelates (aquo-(E)-(((l1-oxidaneyl)dioxo-l-6-sulfaneyl)oxy)((1-(((4,6-dimethylpyrimidin-2-yl)imino)methyl)naphthalen-2-yl)oxy)iron and aquo-(E)-acetoxy((1-(((4,6-dimethylpyrimidin-2-yl)imino)methyl)naphthalen-2-yl)oxy)zinc) were synthesized following an alreadyreported synthetic procedure[14] as presented in schemes 1 and 2 below.The uncorrected melting points via a digital melting point device were acquired. Synthesized compounds were evaluated by assessment of spectral (UV-Visible, NMR, ESI-MS, FT-IR); analytical andmelting point values with comparableliteraturereports. The absorbance wavelength wasobtained throughon a Perkin Elmer Lambda 40 UV–Vis spectrometer with a quartz cuvette. The FT-IR spectra (50-4400 $cm^{-1}$) were acquired on a Bruker alpha-P FT-IR spectrometer adoptingdehydratedKBr as reference. Microanalyses stoodacquiredvia an ElementarVario-EL-Cube set-up for CHNS evaluation. A Gouy magnetic balance was adopted for magnetic susceptibility determination of the metallic chelates at 27$^oC$.

### 2.3THE EXTRACTION PROCESS

The extraction of the metallic species from the aqueous phase into organic phase (portion) using the recently synthesized chelator-ligand wasexaminedvia solvent extraction. 20 mL of aqueous solutions comprising 0.0017M of the metallic acetate salts remained equilibrated with equal volume of chloroform consisting of0.00045M of the chelator-ligand by stirringforcefully at 27$^oC$ on a motorized-shaker for 2-

hrs.This was followedby careful transfer of the solution into a separatory funnel allowed to stand for ½-hr to establish equilibrium. The aqueous portion was then separated from the organic portionwith concentration of metallic ions determined in both phases via atomic adsorption spectrophotometer (AAS). The extraction efficiency, E (%) was acquired according toEq. 1[15].

$$E\ (\%) = \frac{D}{D + \frac{A}{O}} \times 100 \quad \text{————(1)}$$

The solvent extraction procedures could be described by Eq. 2 in which metallic ion ($M^{n+}$) forms a chelate with the chelator-ligand (LH) to afford a neutral structural assemblage ($ML_x$).

$$M^{n+}(aq) + xHL(org) \rightleftharpoons ML_x(org) + nH^{+}(aq) \text{ ————————} (2)$$

The mechanism of extraction correlates with a cation interchange where a complex of stoichiometric formula $ML_x$ is established in the organic phase producing n mol of $H^+$ in the aqueous phase. Hence, the extraction constant ($K_{ext}$) can be stated as;

$$K_{ext} = \frac{[ML_x]_{(org)}\,[H^+]^n_{(aq)}}{[M^{n+}]_{(aq)}\,[HL]^x_{(org)}} \text{————————————————(3)}$$

Since the metallic ion $M^{n+}$ is predominant in the aqueous phase and $ML_x$ is the only extractable specie, the distribution ratio, *D* can be calculated following Eq. 4. The D is used as the most imperative index for determining the adeptness of a solvent extraction procedure.

$$D = \frac{[ML_x]_{(org)}}{[M^{n+}]_{(aq)}} = \frac{\text{Metal ions concentration in the organic portion}}{\text{Metal ions concentration in the aqueous portion}} \text{————(4)}$$

## 2.4 BIOLOGICAL STUDIES

Anti-bactericidal evaluation of the Fe(II) and Zn(II) chelates alongside their chelator-ligand were obtained via an agar well diffusion technique[16] with DMSO as reaction medium. The bacteria strains, reference drugs and procedural stepsreported in our previous study[17] were adopted with the sole aim of finding the most active compound with the best antibacterial potentials.

A disc evaluativepractice was adopted in-vitro to appraise the anti-fungoid actions of the chelator-ligand and its metal-chelatesagainst*A. niger, A. flevus*and *R. Stolonifer*. Potato dextrose agar (PDA) served as medium for the harvest of matured conidia of fungal isolates which were suspended in ringer solution. A 1 mL conidial suspension for a separatefungoid isolate was inoculated on a petri dish of 90 mm with 20 mL PDA. The chelates with the chelatorin DMSO were dissolved (10 mg/mL, 5 mg/mL and 1 mg/mL). Bored germ-free 7mm diameterdisc holes were filled(0.15 □L)with individual test compound's solution and experimental data acquiredin duplicate at three altered concentrations. Fluconazole as adopted as reference drug while DMSO stood as the negative control. The inhibition growth zoneswereevaluated after 24 h and expressed as the inhibition zone in mm.

## 2.5 QUANTUM CHEMICALCALCULATION (QCC)

The chelatorforappraisalremainedevaluatedviaDFT, adopting Becke's 3-parameter hybrid interchange function fused to Lee-Yang-Parr correlation functional (B3LYP) by means of6-311G++(d,p) simple set. AllQCCs stoodcompleted adopting Gaussian-9-package. Optimized structural geometry as well as visualization into HOMO plus LUMO calculations remained acquired via gauss-View 5.0.8 package enablingthe determination of other parameters.With Molinspirationcheminformatic, all pharmacokinetic

factorsstoodacquired for prediction ofbioactivities of the chelatorthough the property explorer appraisalaffordedrelevant dataon the relative cytotoxicity of the chelator.

## 3.RESULTS AND DISCUSSION

### 3.1SYNTHESIS AND PRELIMINARY INVESTIGATIONAL DATA

The synthesized chelates with their chelator-ligand exhibited various shades of colour (Table 1). The $[Fe(L)(B)(SO_4)].H_2O$ and $[Zn(L)(B)(OAc)].H_2O$ chelates displayed shades of brown and yellow separately, while the HL adopted a bright yellow shade. Distinct and sharp melting points different from that of the starting materials were generally obtained for all synthesized compounds (Table 1).Excellentcorrelations were observed amidacquired experimental and calculated values for percentage metallic ratiosdetermined through complexometric titration method as presented in table 1. The molar conductance values (Table 1) of the chelates obtained in dimethylsulphoxide (DMSO) were between9.7–12.0 $Ohm^{-1}mol^{-1}cm^2$ indicative of non-ionic statusfor the soluble chelates. The latter arises from literature reportswhich affirms that values of 45-90 $Ohm^{-1}mol^{-1}cm^2$and 90-120 $Ohm^{-1}mol^{-1}cm^2$ are generally for 1:1 and 1:2 ionic chelates[22]. The molar conductance dataremainedintenselyvalidated by the micro (CHNS) plus quantitative analyses data in which no anions were noticed. The solubility tests of the chelator and its chelates obtained in polar and non-polar organic solvents gave varied solubilities (Table 2). The compounds were majorly or slightly insoluble in $H_2O$, $CH_2Cl_2$ and $CH_3NO_2$. Moreover, the compounds had good solubilities in chloroform, dimethylsulfoxide and dimethylformamide but were sparingly soluble in ethanol, methanol and dichloromethane. The chelator and chelates had moderate-good (46-59%) yields (Table 1). The micro analysis, C, H, N,S data for the chelator and its chelates shown in table 1 have been obtained and the values remains consistent with the theoretical values corroborating 1:1:1 stiochiometries for the heteroleptic chelates and conforms with the empirical formula suggested for each compound

**Table 1. Analytical data for HL Chelator-ligand plus its heterolepticFe(II) and Zn(II) Chelates**

| Molecular Formula | Formula Weight (g/mol) | Colour | Melting Point ($^oC$) | Yeild (%) | $\mu_{eff}$ (B.M) | Molar Conductance ($Ohm^{-1}Mol^{-1}cm^2$) | Analytical/Found (Calculated) % | | | | |
|---|---|---|---|---|---|---|---|---|---|---|---|
| | | | | | | | C | H | N | S | M |
| HL | | | | | | | 73.94 | 5.53 | 15.41 | - | - |
| $C_{17}H_{15}N_3O$ | 278.86 | Yellow | 194-196 | 59.30 | - | - | (73.89) | (5.47) | (15.23) | - | - |
| B | 156.18 | White | 63-66 | - | - | - | - | - | - | - | - |
| $[Fe(L)(B)(SO_4)].H_2O$ | | Redish | | | | | 53.99 | 4. 05 | 11.68 | 5.52 | 9.56 |
| $[FeC_{27}H_{22}N_5O_5S].H_2O$ | 602.368 | Brown | 319-321 | 46.00 | 4.97 | 12.08 | (53.83) | (4.02) | (11.63) | (5.32) | (9.27) |
| $[Zn(L)(B)(OAc)].H_2O$ | | Bright | | | | | 60.64 | 4.83 | 12.22 | - | 11.44 |
| $[ZnC_{29}H_{25}N_5O_3].H_2O$ | 574.676 | Yellow | 289-291 | 51.30 | 0.24 | 9.71 | (60.60) | (4.74) | (12.19) | - | (11.38) |

***Key**: B = 2,2'-Bipyridine; $SO_4$ = Sulphate; OAc = Acetate; $\mu_{eff}$= Effective Magnetic Moment Value; B.M = Bohr Magneton*

**Table 2. Solubility results of HL Chelator-ligand and its heterolepticM(II) Chelates**

| Compound | Distilled $H_2O$ | MeOH | EtOH | $CH_2Cl_2$ | $CHCl_3$ | DMSO | DMF | $CH_3NO_2$ |
|---|---|---|---|---|---|---|---|---|
| HL | SS | SS | S | SS | S | S | S | SS |
| $[Fe(L)(B)(SO_4)].H_2O$ | SS | S | S | SS | S | S | SS | SS |
| $[Zn(L)(B)(OAc)].H_2O$ | SS | SS | SS | SS | SS | SS | SS | SS |

***Key:** S=Soluble; SS=Slightly Soluble; NS=Not Soluble*

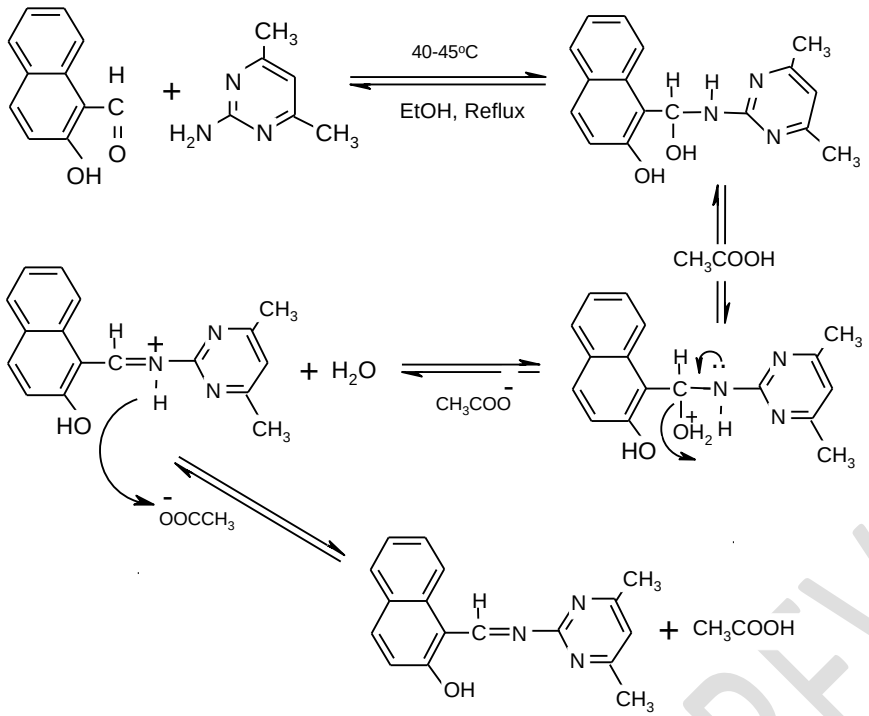


**Scheme 1.Synthetic Procedure for the Chelator-Ligand**

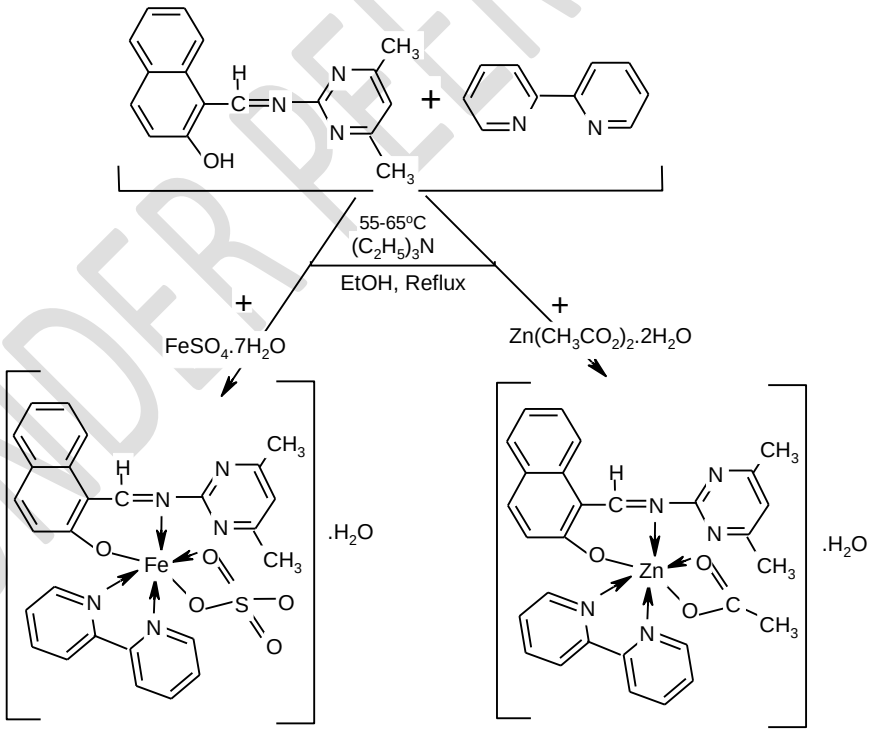


**Scheme2.Synthetic Diagram and Proposed Structure for the Metallic Chelates**

### 3.2EXTRACTION OF METALLIC IONS USING THE SYNTHESIZED CHELATOR-LIGAND

The extraction proficiencies of the chelator-ligand were evaluated by means of solvent extraction on $d^6$ and $d^{10}$ metallic ions ($Fe^{2+}$ and $Zn^{2+}$) into chloroform under neutral conditions. The table 3 below illustrated the number of metallic ions in the aqueous as well as organic phases after the extraction in addition to the extractability of the chelator-ligand.

**Table 3. Extraction Efficiency of HL Chelator-Ligand**

| Metallic ion | Aqueous phase (mg/L) | Organic phase (mg/L) | Distribution ratio | Percentage extraction (%) |
|---|---|---|---|---|
| $Fe^{2+}$ | 0.8201 | 3.1454 | 3.84 | 79.34 |
| $Zn^{2+}$ | 0.0682 | 0.0734 | 1.08 | 51.92 |

From the extraction data presented in table 3, it was noticed that the chelator displayed high extractability for $Fe^{2+}$ with extraction efficiency of 79.34%, and showed a fair extractability potential for $Zn^{2+}$ with extraction efficiencies of 51.92%. The chelator-ligand exhibited moderately good extractability for the metallic ions.

### 3.3NMR STUDIES

The $^1$H-NMR spectrum of the chelator-ligandwas shown Fig. 4and its signal positions presented in table 4a. The methyl protons on the pyrimidine ring gave sharp singlet peak around 3.34 ppm while the $C_5$proton resonated around 6.65 ppm. Equally, the protons ($H_{15}$, $H_{16}$, $H_{17}$ and $H_{18}$) of the napthalene ringappeared as twofold-signals around 7.83-7.84, 7.10-7.29, 7.50-7.53 as well as 7.64-7.66 ppm in addition to lone-signals ($H_{11}$ and $H_{12}$) around 8.03 ppm plus 7.31 ppm separately. The signals around 14.42 ppm plus 9.55 ppm were corroborated the phenolic proton plusC=N proton in the chelator-ligand spectrum. The lattervalidates the existence of OH as well as formation of the chelator. The $^{13}$CNMR spectrum (Figure 5) displayed resonance signals (Table 4b) characteristic of napthalene $C_{11}$-$C_{20}$ atoms at 108.06, 133.7, 129.2, 129.5, 126.3, 124.5 ppm and 119.3 ppm singly. The signal at 141.3 remained consistent of the azomethineC-atom ($C_{10}$), while detected signals around 183.8 ppm, 168.7 ppm as well as 116.8 ppm remainedseparatelyascribed to $C_2$, $C_{4,6}$plus $C_5$ atoms of the pyrimidine function. Consequently, $C_{7,8}$appeared as lone signal around 23.44 ppm.

**Table 4a.$^1$Hnmr data of the synthesized Chelator-ligand, HLin ppm**

| Chelator | $C_{10}H_6$ | $C_4H_6$-$N_2$ | $C_{10}H_4$-$O_2$ | HC=N | O-H | $CH_3$ | N-H |
|---|---|---|---|---|---|---|---|
| HL $C_{17}H_{15}N_3O$ | 7.10-7.84 | 6.65 | - | 9.55 | 14.42 | 3.34 | - |

**Table 4b.$^{13}$Cnmr data of the synthesized Chelator-ligand, HL**

| Chelator | $C_{10}H_6/C_8H_5$ | $C_4H_6$-$N_2$ | [-C=O (-one)]$_2$ | HC=N | $CH_3$ |
|---|---|---|---|---|---|
| HL $C_{17}H_{15}N_3O$ | 108.06-133.7 | 116.8-183.8 | - | 141.3 | 23.44 |

### 3.4FT-IRDATA

The FT-IR spectrum of the chelator-ligandpresented no bands arising from amino groups as noticed within the spectrum of the precursor amine adopted for synthesis indicative of condensation via the amino group with the aldehyde[18]. Acquired spectral bands necessary for structural estimations for the synthesized compounds are presented in table 5. The broad to medium band centered at 3440 cm$^{-1}$remainedapportioned to intra-proton-bonding vibrations (*v*O-H….N) of an enolassemblagefrequently detected in chelators consisting ofterminal OHfunctions. The band remained absent in the spectra of the chelates validating chelation via the naphthol oxygen atom of the chelator. Though, observed medium-broad bandsfrom3348 cm$^{-1}$-3447 cm$^{-1}$in the spectra of metallic chelates remainedattributed to *v*OH of coordinated/hydrated water molecules[11]. While the sharp-medium H-stretching bands of the aromatic rings, v(Ar–H), within the chelator appeared amid 3013-3001 cm$^{-1}$,the chelates displayed medium asymmetric plus symmetric stretching vibrations for the alkyl groups within 2929-2913 cm$^{-1}$. The absorption band at 1628 cm$^{-1}$ due to C=N moiety moved to lower/higher frequencies in the chelates to the range 1614-1667 cm$^{-1}$, substantiatingparticipation of the azomethine*N*in chelation with the M(II) ions[12]. The new band, C=N in addition tothe cyclic C=C vibrations almost appeared at equal strength in the chelatorfrom 1628 cm$^{-1}$to 1593 cm$^{-1}$ but were observed at lower/higher frequencies by ±30cm$^{-1}$in the chelates. The C=N function was apportioned to participation of the imine *N* in interaction with the M(II) ions, while the C=Cwas a consequence of aromatic conjugations plus the effect of chelation[19, 20]. The status of *v*(C=N) remained same(single) in the spectra of all compoundssuggestive of Fermi resonance[12, 21].On the other hand, the band around 1290 cm$^{-1}$within the chelator's spectrum was accredited to *v*(C-O) which displayed significant shifts to greater/lesserfrequencies in the spectra of the chelatesowing to chelation. The sharp band in the spectrum of the chelator observed at 981 cm$^{-1}$ was due to *δ*CH. The *δ*CH band still appeared prominent in the chelates nonethelessmoved to greaterwavenumbers (977-830 cm$^{-1}$). The M-N and M-O bands were detected around 594-547as well as 452-451 cm$^{-1}$separately, confirming chelation via the imine *N* and enol*O* atoms.

**Table 5.Infrared spectral ($cm^{-1}$) data of the Chelator-ligand with its heteroleptic Chelates**

| Compounds | *v*(OH) | *v*(C=N) | *v*(C=C) | *v*(C-N) | *v*(C-C) | *v*(C-O) | δC-H | M-N | M-O |
|---|---|---|---|---|---|---|---|---|---|
| HL | 3441 | $1628_s$ | $1593_s$ | $1537_s$ | $1432_s$ | $1290_s$ | $981_s$ | - | - |
| B | - | $1639_s$ | $1580_s$ | $1453_s$ | $1349_s$ | - | $991_s$ | - | - |
| $[Fe(L)(B)(SO_4)].H_2O$ | 3439 | $1614_s$ | $1574_s$ | $1529_s$ | $1345_m$ | $1185_m$ | $985_s$ | $547_m$ | $451_m$ |
| $[Zn(L)(B)(OAc)].H_2O$ | 3434 | $1619_s$ | $1589_m$ | $1532_s$ | $1334_m$ | $1188_s$ | $835_m$ | $594_m$ | $452_m$ |

b = broad

Key: *b = broad, s = sharp, d = doublet and m = medium*

### 3.5UV-VIS AND MAGNETIC SUSCEPTIBILITY STUDIES

The UV-Vis spectra of the chelates with their chelator (Table 6) were acquired[7, 22] amid 19000-90000 $cm^{-1}$. Absorption signals remains the outcome of transitions of electrons within the chelator's molecular orbitals (n→π*, π→π*), metallic *d-d* transitions as well as charge transfer (CT) transitions (M→L plus L→MCT)[22]. The absorption signals centered at 29019 $cm^{-1}$within the chelator's spectrum exhibited significant shifts in the chelates conforming to n→$\pi*$transition of the C=N functions. Also, the transition $\pi \rightarrow \pi*$ of the chelator observed at32362 $cm^{-1}$ remained almost unaltered in the spectra of the chelates.The signals amid 26607-44052 $cm^{-1}$ in the iron chelate were characteristic of$\pi^* \leftarrow$n, $\pi^* \leftarrow \pi$plusCT transitions. The visible signals at 22727 $cm^{-1}$ (140 L $cm^{-1}$ $mol^{-1}$) and 18904 $cm^{-1}$ (170 L $cm^{-1}$ $mol^{-1}$) remain*d-d*signals apportioned to UV-Vis transitions of$^5T_{2g} \rightarrow {}^5A_{1g}$, and $^5T_{2g} \rightarrow {}^5B_{1g}$separately characteristic of an bivalent iron chelate with octahedral geometry[23-25]. The synthesized ironchelate exhibited magnetic momentat 4.97 B.M. consistent with assigned geometry[26].The spectrum of the bivalent zinc chelate expectedly presentedCT transitions(M→L) at 13123 $cm^{-1}$ and 23419 $cm^{-1}$ as no *d-d* transition was anticipated for $d^{10}$ zinc chelates[27]. The signals at 26290 $cm^{-1}$ and 31949 $cm^{-1}$were typical of intra-chelatorsignals. Bivalent zinc chelates holds $3d^{10}$ electron arrangementbesidesdisplays magnetic moments of almost zero unpaired electrons. Acquired $\mu_{eff}$of 0.24 B.M. denotes diamagnetism for the Zn(II) chelateas well asvalidatesits geometry

**Table 6. Electronic spectra data for the Chelator-ligand plus its heterolepticM(II) Chelates**

| Compounds | Absorption Bands ($cm^{-1}$) | Bands Assignment | Tentative Geometry |
|---|---|---|---|
| HL | 32362 | π – π* | - |
| | 29019 | n – π* | |
| | 44052 | C.T | |
| | 39682, 30769 | π – π* | |
| $[Fe(L)(B)(SO_4)].H_2O$ | 26607 | n – π* | Octahedral |
| | 22727 | $^5T_{2g} \rightarrow {}^5A_{1g}$ | |
| | 18904 | $^5T_{2g} \rightarrow {}^5B_{1g}$ | |

| | | | |
|---|---|---|---|
| | 31949 | π→π* | |
| [Zn(L)(B)(OAc)].$H_2O$ | 26290 | n→π* | Octahedral |
| | 23419 | M→L | |

## 3.6The ESI-MS Studies

The ESI-mass spectrum (Figure 6) of the chelator-ligand presenteddual pathways of disintegration with a base peak m/e+ at 278.12 conforming to the estimated molecular weight (278.85) for the chelator-ligand (Table 7). This substantiates the formation of form HL chelator from 2-hydroxy-1-napthaldehyde plus 2-amino-4,6-dimethylpyrimdine. The signals at m/z 250.17, 193.66 plus 142.92 were arising fromloss of COH, $NC_2H_2O$ and $C_2N_2H$ components while the peak at m/z 124.81 remainedundoubtedlydue to OH lost separately. Additionally, the spectrum had L+1 peak at m/z 279.24, a smallstrength peak at m/z 280.11 which can be ascribed to additional mass units, a result of C-13 existenceas well asextraaverage peak around 276.12 owing to lose of protons

**Table 7. Mass spectra result for the Chelator-ligand**

| Ligands | Fragmentation | |
|---|---|---|
| | m/e | m/z |
| HL $C_{17}H_{15}N_3O$ [278.86] | 278.12 | 279.24 [m+1], 280.11 [m+2] 276.12 [-$H_2$, 2.016], 250.17$[COH]^+$, 193.66$[NC_2H_2O]^+$, 142.92$[C_2N_2H]^+$, 125$[OH]^+$ |

***Keys*:** EMU=Extra mass unit

### 3.7BIOLOGICAL EVALUATIONS

Acquired antibacterial studies data are accessible in table 8 below. From the table, it is obvious that theheterolepticFe(II) and Zn(II) chelates were largely sensitive with varying degrees of inhibitory impacts on the growth of the screened organisms compared to the ligands ('L and B'); a consequence of chelation[13, 14]. Also as observed from the data, the enhanced sensitivity of the chelates with their chelator against the gram positive stains than the gram negative microbes is explainable on the basis of differences in the cell-wall compositions of the microbes as well as the alteration in the penetrability plus permeation of the compounds through the microbial cell membranes[22]. The over-all inhibition of the microbes by the chelator with inhibitory zones of 12.0-19.0 mm could be attributable to the presence of π-electrons within the cyclic moieties as well as the C=Nfunctions frequentlyacknowledged to improve antibacterial actions[28,29]heterocyclic assemblages. TheFe(II) chelatedemonstrated inhibitory growth effect better than that of the chelators ('L' and 'B') against only *B. cereus*(19.5 mm) and*S.aureus*(21.0 mm)indicating its potential significance in new antibacterial drug designs. Though the Zn(II) chelate remained moderate in its actions against the tested microbes. The latter may be assigned to creation of persuasive protein poisons within the cell-surfaces of the microbes averting further penetration of the Zn(II) chelate into the inner portions of the microbial cells as well as imposing lessened lipophilicity of same chelate which automatically reduces permeation into the lipid cell membrane of the microbes[20,30]. The antifungal activities of HL chelator-ligand and itsasymmetrical metallic chelates against *A. niger, A.*

*flevus*and *R. Stolonifer*are contained in Table9. The chelator-ligandhad activity against all the tested

| Compound/Bacteria | A | B | C | D | E | F |
|---|---|---|---|---|---|---|
| HL | 17.5±2.1 | 17.0±2.8 | 15.0±0.0 | 12.0±2.8 | 19.0±1.4 | 14.0±2.8 |
| B | 15.5 ± 0.7 | 12.0 ± 2.8 | 26.0 ± 2.8 | 8.5 ± 0.7 | 17.0 ± 4.2 | 19.5 ± 2.1 |
| $[Fe(L)(B)(SO_4)].H_2O$ | 19.5±3.5 | 15.5±0.7 | 18.0±1.4 | 9.0±1.4 | 21.0±2.8 | 18.5±2.1 |
| $[Zn(L)(B)(OAc)].H_2O$ | 16.0±0.7 | 14.0±2.8 | 8.5±0.7 | 12.0±1.4 | 14.5±0.7 | 13.5±0.7 |
| $^{+}$Ciprofloxacin | 33.0 ± 3.5 | 32.0 ± 1.4 | 36.0 ± 2.8 | 26.5 ± 0.7 | 29.0 ± 2.1 | 23.0 ± 1.4 |
| -DMSO | 0.0±0.0 | 0.0±0.0 | 0.0±0.0 | 0.0±0.0 | 0.0±0.0 | 0.0±0.0 |

speciesexcept *R. Stolonifer*which showed resistance. The Fe(II) and Zn(II) chelates were suggestively active against *A. flevus*and *A. niger*onlywith inhibitory zones of 15.0 - 21.0 mm.

**Table 8.Antibacterial data of HL Chelator-ligand and its heterolepticM(II) Chelates**

**Key:** A= *B. cereus; B = E. coli;* C = *K. oxytoca;* D = *P. aeruginosa; E =S.aureus; F= P. mirabilis*

**Table 9. Antifungal result for the Chelator-ligand and its M(II) Chelates**

| Fungal/Compounds | G | H | I |
|---|---|---|---|
| HL | 19±1.4 | 21±0.7 | - |
| B | 16±1.6 | 19±1.4 | 13±0.7 |
| $[Fe(L)(B)(SO_4)].H_2O$ | 15±1.4 | 17±0.0 | - |
| $[Zn(L)(B)(OAc)].H_2O$ | 17±2.1 | 21±0.0 | - |
| $^{+}$ Fluconazole | 36±0.3 | 29±0.7 | 38±0.3 |
| -DMSO | - | - | - |

**Key: G = *A. niger;* H = *A. flevus;* I = *R. Stolonifer***

### 3.8ANTIOXIDANT STUDIES

The chelator-ligand with its $M^{2+}$ chelates were appraised for radical scavenging actions using DPPH (1,1-diphenyl-2-picryl-hydrazyl) radical at 200, 100 plus 50$\mu$g/mL concentrations in 1mL DMSO. Acquired dataon the basis of percentage inhibition are obtainable in Table 10. A goodanalysis of the datadesignates that the chelator plus its chelateslargelydemonstratedradical scavenging actions in DPPH assay. Inhibitory values commonly reflect degree of radical scavenging actions. The chelator-ligandsubstantivelyexhibited percentage inhibitory values smaller or comparable to that of standardsuggestive of its anti-oxidant abilities. The potentials of the chelator-ligandgot enhancednoticeablyon chelation with M(II) ions. Largely, the metallic chelates presentedsuperior DPPH radical scavenging actions. Subsequently, the data of the DPPH antioxidant actions attested that the compounds could be adopted for design as well as syntheses of drugs for the management of pathological illnessesrising from oxidative stress.

**Table 10**.**Antioxidant Data for the Chelator-ligand and its heterolepticFe(II) and Zn(II) Chelates**

| Compounds | Concentration | Absorbance | | | Mean(Error) | % Inhibition (Error) |
|---|---|---|---|---|---|---|
| | | 1 | 2 | 3 | | |
| Blank | - | 0.77 | 0.78 | 0.78 | - | - |
| HL | $Ic_{50}$ | 0.09 | 0.09 | 0.09 | 0.58(±0.001) | 86.56(±0.07) |
| | $Ic_{100}$ | 0.088 | 0.083 | 0.083 | 0.585(±0.003) | 87.33(±0.46) |
| | $Ic_{200}$ | 0.082 | 0.078 | 0.079 | 0.590(±0.002) | 88.1(±0.36) |
| B | $Ic_{50}$ | 0.172 | 0.170 | 0.168 | 0.501(±0.004) | 74.76(±0.570) |
| | $Ic_{100}$ | 0.160 | 0.160 | 0.158 | 0.510(±0.002) | 76.23(±0.234) |
| | $Ic_{200}$ | 0.152 | 0.152 | 0.150 | 0.518(±0.002) | 77.40(±0.173) |
| $[Fe(L)(B)(SO_4)].H_20$ | $Ic_{50}$ | 0.167 | 0.167 | 0.168 | 0.502(±0.001) | 75.03(±0.07) |
| | $Ic_{100}$ | 0.092 | 0.092 | 0.092 | 0.578(±0.001) | 86.26(±0.07) |
| | $Ic_{200}$ | 0.050 | 0.057 | 0.050 | 0.617(±0.004) | 92.16(±0.57) |
| $[Zn(L)(B)(OAc)].H_2O$ | $Ic_{50}$ | 0.024 | 0.018 | 0.019 | 0.649(±0.004) | 96.96(±0.49) |
| | $Ic_{100}$ | 0.005 | 0.011 | 0.014 | 0.66(±0.003) | 98.53(±0.71) |
| | $Ic_{200}$ | 0.006 | 0.004 | 0.002 | 0.666(±0.003) | 99.4(±0.30) |
| Standard Ascorbic Acid | $Ic_{50}$ | 0.093 | 0.089 | 0.094 | 0.578(±0.002) | 86.26(±0.38) |
| | $Ic_{100}$ | 0.085 | 0.081 | 0.082 | 0.587(±0.002) | 87.66(±0.32) |
| | $Ic_{200}$ | 0.078 | 0.074 | 0.076 | 0.594(±0.002) | 88.67(±0.35) |

### 3.9QUANTUM CHEMICAL STUDIES

The Frontier Molecular orbital allows for the prediction of reactivity of the chelator whose active site could be established by the distribution of the orbital frontiers. The HOMO is seen as a nucleophile, while LUMO. The LUMO is seen as an electrophile which accepts electrons from nucleophile. Several chemical reactivity descriptors, such as the chemical potential, global hardness and electrophilicity, have been calculated and is presented in table 11

**Table 11.Quantum chemical parameters of Chelator-Ligand, HL**

| PARAMETER | |
|---|---|
| Energy (ev) | -24255.97417444094 |
| E- lumo | -1.7179 |
| E- homo | -5.9163 |
| Energy gap | 4.1984 |
| Dipole moment (Debye) | 3.4824 |
| Ionization potential | 5.9163 |
| Electron affinity | 1.7179 |
| Electronegativity | 3.8171 |

| | |
|---|---|
| Hardness | 2.0992 |
| Softness | 0.2382 |
| Electrophilicity | 3.4703 |

Theglobal reactivity and local descriptors remainedevaluated viaKoopman's theorem equations expressed as:

Ionization potential(I) = -E-homo

Electron affinity(A) = -E-Lumo

Electronegativity (χ) = (I +A)/2

Hardness (η) = (I – A)/2

Softness (S) = 1/2 η

Electrophipilicity(ω) = μ2/2η

where μ which is chemical potential is - χ

Low energy gap value denotes high chemical reactivity[31], while high energy gap signifies low chemical reactivity. The energy gap of the chelator was observed to be low which suggested high chemical reactivity. Theelectrophilicity is a measure in stabilization of energy when a compound accepts an extra electronic charge withinits environ. Often perceived animproved descriptor of general chemical reactivity consisting oftogether the capacity of an electron-loving specie to obtain an extra electronic charge as well as the non-acceptance of a compound to undergo an electronic charge interchange in its environ. It offersbasic facts on electron transfer (chemical potential) and stability (hardness). The 'χ'ascertainsthe attraction of electrons to an atom within a covalent bond. When two dissimilar atoms are bonded covalently, the shared electrons will be more strongly pulled towards the more electronegative atom[32]. The optimized, HOMOin addition to LUMO orbitals of our synthesizedchelator are given belowas figures 1-3 separately.

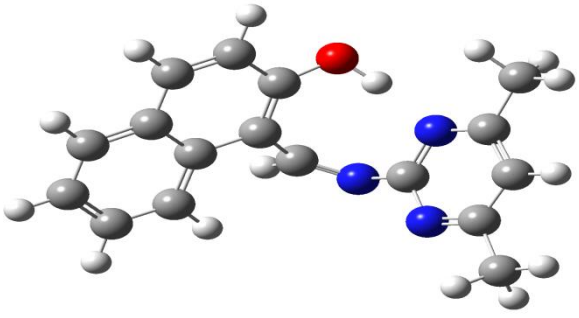

**Figure 1. Optimized Structure of HL Chelator**

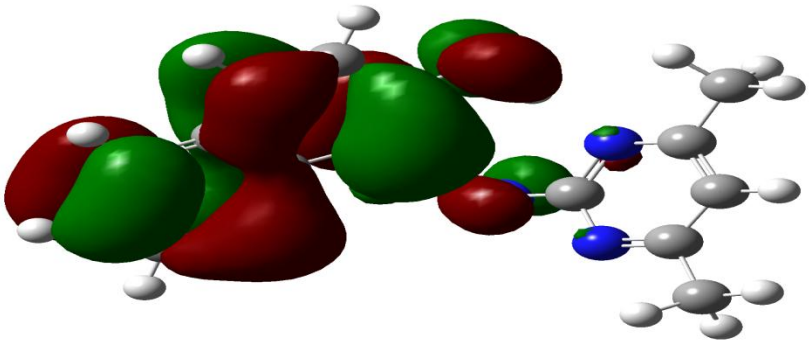

**Figure 2. HOMO ofHL Chelator**

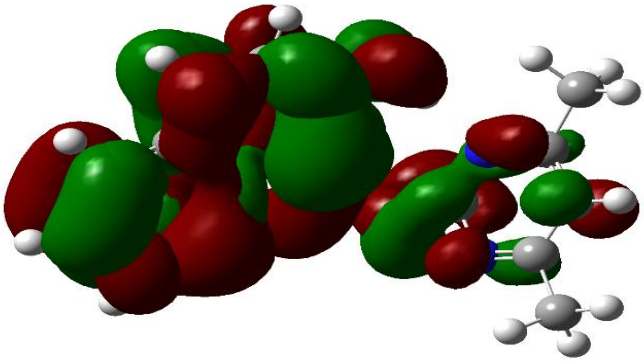

**Figure 3. LUMO of HL Chelator**

The result as presented in table 12 showed that the chelator'spharmokinetic parameters where within the Lipinski rule of five. This entails that the chelator will be of good oral bioavailability. A bioactivity score of more than 0 signifies a chelator's activeness. Between -0.5–0, it is moderately active and a value less than -0.5 suggests inactiveness. Table 13 shows the bioactivity scores of the chelator. Except for its enzyme inhibitor and Kinase inhibitor probability scores which fell within the moderately active zone. The chelator showed values that suggests inactivity for the remaining drug-likeness parameters. The risks of toxicity (mutagenicity, tumorigenicity, irritation, reproduction) as well as the physicochemical features (miLogP, solubility, drug likeness plus drug score) remainedevaluated viaaprocedureestablished by property explorers and illustrated in table 14. The cLogp and the solubility were observed to be within the acceptable criteria. , which suggested good absorption and distribution (Lotfy, 2015).

**Table 12.Molecular Properties Descriptors**

| PHARMOKINETIC PARAMETERS | | | | | | | |
|---|---|---|---|---|---|---|---|
| Vol | TPSA | Nrotb | HBA | HBD | LogP | MW | Violation |
| - | - | - | < 10 | < 5 | ≤ 5 | < 500 | ≤ 1 |
| 255.33 | 58.38 | 2 | 4 | 1 | 3.63 | 277.33 | 0 |

***Vol.*** *volume;* ***TPSA.*** *Topological polar surface area;* ***NROTB.*** *number of rotatable bonds;* ***HBA****. number of hydrogen bond acceptors;* ***HBD****. number of hydrogen bond donors* ***Log P****. logarithm of compound partition;* ***MW****. molecular weight*

**Table 13.Bioactivity Score according to MolinspirationCheminformaticsSoftware**

| DRUG-LIKENESS | | | | | |
|---|---|---|---|---|---|
| GPCR | ICM | KI | NRL | PI | EI |
| -0.53 | -0.75 | -0.42 | -0.52 | -0.66 | -0.26 |

*GPCR ligand. ICM: Ion channel modulator, KI: Kinase inhibitor, NRL: Nuclear receptor ligand, PI: Protease inhibitor, EI: Enzyme inhibitor*

**Table 14. Property Explorer properties of the Chelator-Ligand**

| TOXICITY RISKS | | | | PROPERTY CALCULATIONS | | EXPLORER | |
|---|---|---|---|---|---|---|---|
| MUT | TUM | IRRI | RE | cLogp | S | DL | DS |
| HR | HR | LR | LR | 3.48 | -0.47 | -3.58 | 0.13 |

*HR ; High Risk,LR; Low Risk,MUT : mutagenic ; TUMO : tumorigenic ; IRRI: irritant ; RE: reproductive effective ; CLP: cLogP ; S: Solubility ; DL : Drug-likeness ;DS : Drug-Score.*

## 4. CONCLUSION

The $N_2O_2$ chelator-ligand with its bivalent heteroleptic Fe and Zn chelates were obtained through reflux-condensation reaction. Spectral plus analytical techniques were utilized for the characterization of the synthesized compounds. The deprotonated nitrogen of the amine moiety and carbon of the carbonyl reagent gave rise to the chelator-ligand with $N_2O_2$chromophore detected around the metallic atom of the chelates. The $\mu_{eff}$ data plus UV-Vis spectral values of the chelates conformed to 6-coordinate octahedral geometry and assigned same. All the chelates are high spin and non-ionic in dimethylsulfoxide (DMSO). The antimicrobial screening of the chelates presented moderate to excellent results but with respect to standard drug used, the tested compounds were found to be moderately active.The bivalent heteroleptic chelates demonstrated good scavenging actionslike the standard drug adopted. The chelator-ligand was further evaluated for metallic extractive proficiency and an outstanding extractability for $Fe^{2+}$ and $Zn^{2+}$ions with an efficiency of 79.34% and 51.92% was acquired correspondingly.

## SIGNIFICANT STATEMENT

Reflux-chelative process was unraveled in this study as a synthetic method for an $N_2O_2$ chelator-ligand with an enoltautomeric assemblage. Principally, the study established that the chelates demonstrated

outstanding biological actions over their chelator against tested microbial organisms. However, the metallic ions' extractive potentials of thechelator-ligand as observed remained prospective

## DECLARATION OF CONTENDING INTEREST

Author entirely state here that no contending interest exist anywhere or in any form with regards to the publication of the article.

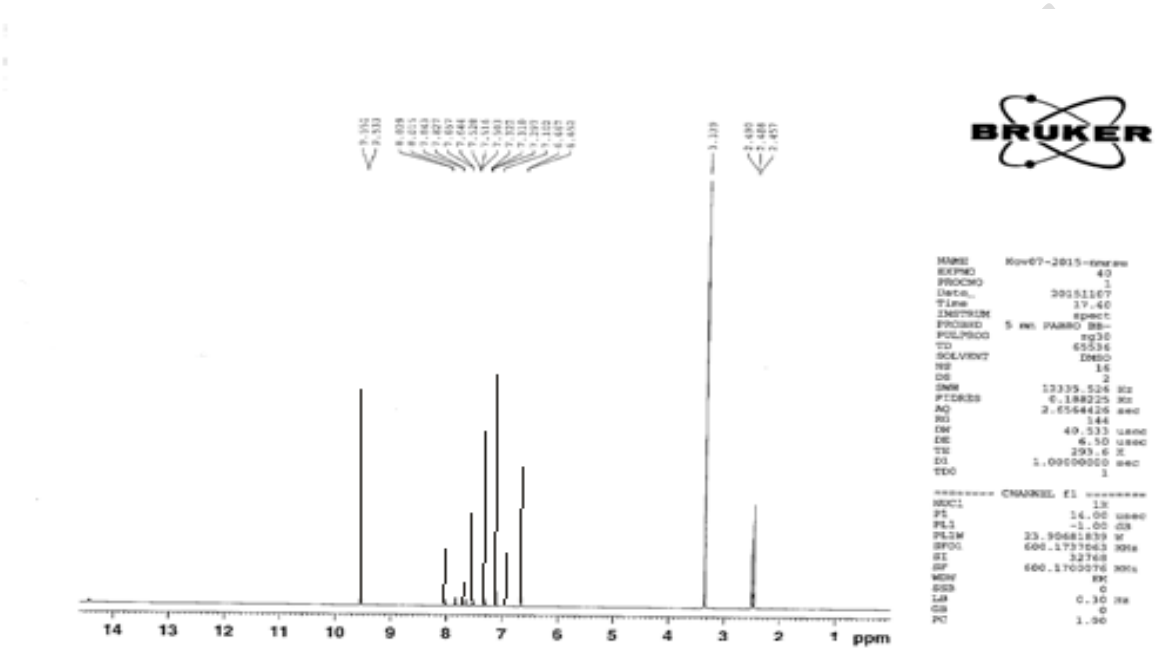


**Figure 4. $^{1}$Hnmr spectrum of the Chelator-ligand**

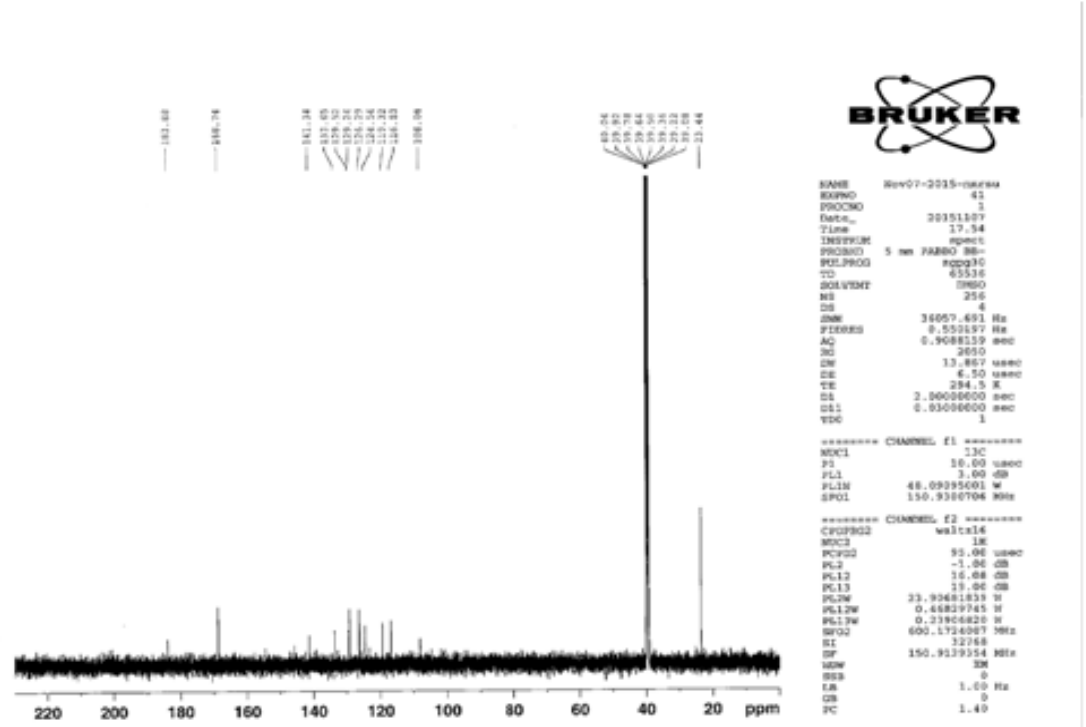


**Figure 5.$^{13}$Cnmr spectrum of the Chelator-ligand**

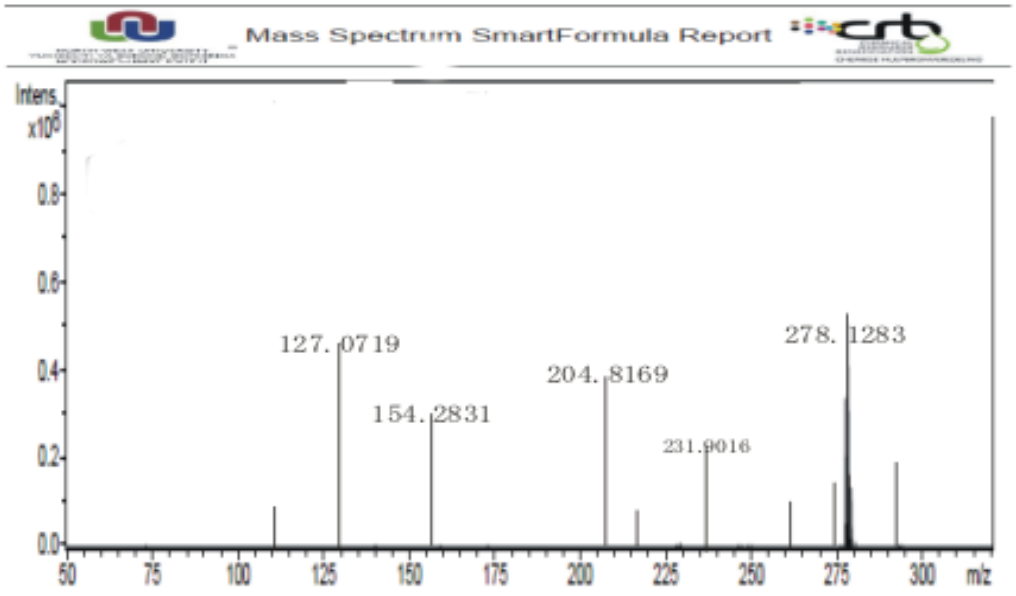


**Figure 6. Mass spectrum of the Chelator-ligand**

## COMPETING INTERESTS DISCLAIMER:

Authors have declared that no competing interests exist. The products used for this research are commonly and predominantly use products in our area of research and country. There is absolutely no conflict of interest between the authors and producers of the products because we do not intend to use these products as an avenue for any litigation but for the advancement of knowledge. Also, the research was not funded by the producing company rather it was funded by personal efforts of the authors.

## REFERENCES


1. Ekennia, A. C., Onwudiwe, D. C. and Osowole, A. A. (2014). Spectral, thermal stability and antibacterial studies of copper, nickel and cobalt complexes of *N*-methyl-*N*-phenyl dithiocarbamate. *J. of Sulfur Chem.*36(1):96-104. doi.org/10.1080/17415993.2014.969731
2. Patrick, G. L. (2005). An introduction to medicinal chemistry. 3rdEdn, Oxford University Press, UK
3. McQuitty R. J. (2014). Metal-based drugs. *SciProg*. 2014;97(1):1-19. doi: 10.3184/003685014X13898980185076. PMID: 24800466
4. Richard, J. F. and Yitzhak, T. (2014). Antibiotics and bacterial resistance in the 21st Century.*PerspectMedicinChem* 6:25–64.doi:10.4137/PMC.S14459
5. Monisha, J., Tenzin, T., Naresh, A., Blessy, B. M. and Krishnamurthy, N. B. (2014). Toxicity, mechanism and health effects of some heavy metals.*InterdiscipToxicol*. 7(2):60–72. doi: 10.2478/intox-2014-0009
6. Glenn, S. T. and Nicolette, T. (2013). New and alternative approaches to tackling antibiotic resistance.F1000Prime Rep2013, **5**:51. doi: 10.12703/P5-51.
7. Festus, C., Ekennia, A. C., Collins, U. I., Okafore, S. N., Onwudiwe, D. C., Osowole, A. A. and Oguejiofo T. U. (2018a). Synthesis, characterization, antimicrobial activity and DFT studies of 2-(pyrimidin-2-ylamino)naphthalene-1,4-dione and its Mn(II), Co(II), Ni(II) and Zn(II) complexes. *J. of Molecular Structure.* 1163 (2018) 455-464; https://doi.org/10.1016/j.molstruc.2018.03.025 0022-2860.
8. Graham, L. P. (2005). An introduction to medicinal chemistry 3rd Edition. Oxford University press, UK .
9. Parveez, G. and Athar, A. H. (2015). Biological activity studies on metal complexes of macrocyclic Schiff base Ligand: Synthesis and spectroscopic characterization. *J. Braz. Chem. Soc* 26(7):1331-1337. doi.org/10.5935/0103-5053.20150099.
10. Samuel, T., David, K. D., Regina, A. and Isaac, T.(2014). Spectroscopic characterization, *In Vitro* cytotoxicity, and antioxidant activity of mixed ligand Palladium(II) Chloride Complexes Bearing Nucleobases. *Journal of Inorganic Chemistry*, 2014,dx.doi.org/10.1155/2014/586131.
11. Osowole, A. A. and Festus, C.(2015). Synthesis, spectral magnetic and antibacterial studies of some divalent metal complexes of 3-{[(4,6-dihydroxy pyrimidin-2-yl)Imino]methyl}Napthalen-2-ol. *Journal of Chemical, Biological and physical sciences,* 6(11); 210-219, *www.jcbsc.org.*
12. Osowole A. A. and Festus, C. (2013). Synthesis, characterization and antibacterial activities of some metal(II)complexes of 3-(-1-(2-pyrimidinylimino)methyl-2-napthol. *Elixir Appl. Chem*59:15843-15847.

13. Tetteh, S., Dodoo, D. K., Appiah-Opong, R. and Tuffour, I. (2014) Spectroscopic characterization, *In Vitro* cytotoxicity, and antioxidant activity of mixed ligand Palladium(II) chloride complexes bearing nucleobases. *J. of Inorg. Chem.,*2014.doi.org/10.1155/2014/586131
14. Festus, C., Ibeji, C.U. and Okpareke, O. (2020). Novel 3d divalent metallic complexes of 3-[(2-hydroxy-5-methylphenylimino)-methyl]-napthalen-2-ol: Synthesis, spectral, characterization, antimicrobial and computational studies. *Journal of Molecular Structure.* 1210 (2020); 1-13.
15. Zoubi, W.A., Kandil, F. and Chebani, M. K. (2012). Synthesis of macrocyclic Schiff bases based on pyridine-2,6-dicarbohydrazide and their use in metal cations extraction. *Organic chemistry Current research*. 1(1); 1-7
16. Chioma, F., Ozioma, A. E. and Don-Lawson, C. D. (2020). Novel metal2+ complexes of N-(1,4-dihydro-1,4-oxonaphthalen-3-yl) pyrazine-2-carboxamide: Synthesis, structural characterization, magnetic properties and antimicrobial activities. *Curr. Res. Chem.,* 12: 1-10
17. Festus, C., Jude, I. A., Collins, U. I. (2021). Ligation Actions of 2-(3-hydroxypyridin-2-ylamino)naphthalen-1,4-dione: Synthesis, characterization, *In-vitro* antimicrobial screening, and computational studies. *Indian J. of Heterocyclic Chemistry*, 31(01); 1-13.
18. Valarmathy, G. and Subbalakshmi, R. 2014. Synthesis, spectral characterisation, electrochemical, and fluorescence studies of biologically active novel Schiff base complexes derived from E-4-(2-hydroxy-3-methoxybenzlideneamino)-N-(pyrimidin-2-yl)benzenesulfonamide. *Turkish Journal of Chemistry* 38: 521-530
19. Jayabalakrishnan, C. and Natarajan, K. (2002). "Ruthenium(II) carbonyl complexes with tridentate Schiff bases and their antibacterial activity," *Transition Metal Chem.,* 27.1: 75–79
20. Festus, C., Anthony, C. E., Osowole, A. A., Lukman O. O., Damian, C. O., and Oguejiofo, T. U. (2018b). Synthesis, experimental and theoretical characterization and antimicrobial studies of some Fe(II), Co(II) and Ni(II) complexes of 2-(4,6-dihydroxypyrimidin-2-ylamino)naphthalene-1,4-dione. *Research on Chemical Intermediates 44(10):5857-5877; DOI 10.1007/s11164-018-3460-7*
21. Kalsi, P. S. (2004). Spectroscopy of organic compounds. 6th Edition. New age International publishers, India 71-7249.
22. Damian, C. O., Anthony, C. E. and Eric, H. (2016). Syntheses, characterization, and antimicrobial properties of nickel(II) dithiocarbamate complexes containing NiS4 and NiS2PN moieties, Journal of Coordination Chemistry, DOI:10.1080/00958972.2016.1186800
23. Salmon, L., Molnar, G., Cobo, S., Oulié, P., Etienne, M., Mahfoud, T., Demont, P., Eguchi, A., Watanabe, H., Tanaka, K. and Bousseksou, A. 2009. Reinvestigation of the spin crossover phenomenon in the ferrous complex $[Fe(HB(pz)_3)_2]$. *New Journal of Chemistry* 33.6: 1283-1289.https://doi.org/10.1039/B902811K
24.Festus, C., Ekpete, O.A. and Don-Lawson, C. D. (2020). Novel metal2+ complexes of N-(1,4-dihydro-1,4-oxonaphthalen-3-yl) pyrazine-2-carboxamide: Synthesis, structural characterization, magnetic properties and antimicrobial activities. *Curr. Res. Chem.,* 12: 1-10. DOI:10. 3923/crc.2020.1.10
25. Cesar, S., Maria, P. and Cristian. T. (2008). Biologically active transition metal chelates with a 2-thiophenecarboxaldehyde-derived Schiff base: Synthesis, characterization and antibacterial properties. *Turkish Journal of Chemistry* 32:487-493.
26. Salmon, L., Molnar, G., Cobo, S., Oulié, P., Etienne, M., Mahfoud, T., Demont, P., Eguchi, A., Watanabe, H., Tanaka, K. and Bousseksou, A. (2009). Reinvestigation of the spin crossover phenomenon in the ferrous complex $[Fe(HB(pz)_3)_2]$. *New J. of Chemistry* 33.6: 1283-1289.
27. Festus, C., Ekennia, A. C., Osowole, A.A., Okafor, S.N., Ibeji, C. U., Onwudiwe, D. C., Ujam. O. T. (2018). Synthesis, characterization, *in-vitro* antimicrobial properties, molecular docking and DFT studies of 3-{(*E*)-[(4,6-dimethylpyrimidin-2-yl)imino]methyl}naphthalen-2-ol and HeterolepticMn(II), Co(II), Ni(II) and Zn(II) complexes. *Open Chem., 2018; 16: 184–200. https://doi.org/10.1515/chem-2018-0020*

28. Nogrady, T. (1988). Medical Chemistry:A biochemistry approach. Oxford University Press, New York.
29. Osowole, A. A. andFagade, O. E. (2007). “Synthesis, characterization and biopotency of some metal(II) *β*-ketoiminates and their mixed-ligand complexes,” *Polish Journal of Chemistry*. 81.12 2039–2048.
30. Thangadurai, T. D and Natarajan, K. (2001). Mixed ligand complexes of ruthenium(II) containing α, β-unsaturated-β-ketoamines and their antibacterial activity. *Transition Met. Chem.,* 26; 500-504.
31. Singhal, S., Khanna, P., and Khanna, L. (2019). Synthesis, DFT studies, molecular docking, antimicrobial screening and UV fluorescence studies on ct-DNA for novel Schiff bases of 2-(1-aminobenzyl) benzimidazole. *Heliyon*, *5*(10), e02596. doi: 10.1016/j.heliyon.2019.e02596
32. Bououden, W., and Benguerba, Y. (2020). Computational Quantum Chemical Study, Drug-Likeness and In Silico Cytotoxicity Evaluation of Some Steroidal Anti-Inflammatory Drugs. *J. Of Drug Delivery And Therapeutics*, *10*(3-s), 68-74. doi: 10.22270/jddt.v10i3-s.4165